Research Article

Jian Yang, Meiyan Wang, Jing Yang, Zhiqiang Chu, Xueling Chen, Xiangwei Wu*, Xinyu Peng*

Calcifying nanoparticles initiate the calcification process of mesenchymal stem cells *in vitro* through the activation of the TGF-β1/Smad signaling pathway and promote the decay of echinococcosis

https://doi.org/10.1515/biol-2022-0503
received May 14, 2022; accepted August 26, 2022

Abstract: The role of the calcifying nanoparticles (CNPs) in the calcification process of the outer cyst wall in hepatic cystic echinococcosis (HCE) remains unknown. CNPs were isolated from the tissues of the patients with HCE. Western blotting, alkaline phosphatase staining, and alizarin staining were performed to detect the cellular calcium ion deposition induced by the CNPs. CCK-8 and flow cytometry assays were conducted to determine the effect of CNPs on the apoptosis of mesenchymal stem cells (MSCs). Western blot experiments were performed to examine the expression levels of apoptosis-related factors and TGF-β1/Smad signaling pathway constituents. Treatment with CNPs induced the differentiation of MSCs. Calcium-related proteins, including OPN, BMP-2, and RUNX2, were upregulated after the CNP treatment. Similarly, CNP exposure increased the cellular calcium ion deposition in MSCs. In addition, the expression of Bax and Caspase-8 was elevated by the CNPs in MSCs. Treatment with CNPs promoted MSC apoptosis and inhibited the MSC growth. The TGF-β1/Smad signaling pathway was also activated after the CNP treatment. This study indicated that CNPs may play a critical role in initiating calcification of the outer cyst wall of HCE and promote the decay of echinococcosis, providing a new strategy for the treatment of hepatic echinococcosis.

Keywords: calcifying nanoparticles, mesenchymal stem cells, hepatic echinococcosis, calcification, apoptosis

*** Corresponding author: Xiangwei Wu,** Department of Hepatobiliary Surgery, The First Affiliated Hospital, Medical College, Shihezi University, No. 107, North Second Road, Shihezi, 832008, Xinjiang, China; Key Laboratory of Xinjiang Endemic and Ethnic Diseases, Ministry of Education, Shihezi University School of Medicine, Shihezi, Xinjiang, 832000, China; NHC Key Laboratory of Prevention and Treatment of Central Asia High Incidence Diseases, First Affiliated Hospital, School of Medicine, Shihezi University, Shihezi, 832000, Xinjiang, China, e-mail: wxwshz@126.com
*** Corresponding author: Xinyu Peng,** Department of Hepatobiliary Surgery, The First Affiliated Hospital, Medical College, Shihezi University, No. 107, North Second Road, Shihezi, 832008, Xinjiang, China, tel: +86-993-2859449, e-mail: pengxinyu0508@163.com
Jian Yang: Center of Hepatic Surgery, Tongji Hospital, Tongji Medical College, Huazhong University of Science and Technology, Wuhan, 430030, China; Department of Hepatobiliary Surgery, The First Affiliated Hospital, Medical College, Shihezi University, No. 107, North Second Road, Shihezi, 832008, Xinjiang, China
Meiyan Wang: Department of Nursing, Shihezi University School of Medicine, Shihezi, 832000, Xinjiang, China
Jing Yang, Zhiqiang Chu: Department of Hepatobiliary Surgery, The First Affiliated Hospital, Medical College, Shihezi University, No. 107, North Second Road, Shihezi, 832008, Xinjiang, China
Xueling Chen: Department of Immunology, Shihezi University School of Medicine, Shihezi, 832000, Xinjiang, China

1 Introduction

Hepatic echinococcosis (HE) is a parasitic disease affecting humans and animals. Hepatic cystic echinococcosis (HCE) is caused by an infection with *Echinococcus granulosus* in the liver [1], and this parasite accounts for more than 90% of all the HCE cases, threatening animal husbandry and human health [2,3]. Surgery is a common treatment modality for HCE, but it causes postoperative complications, and the recurrence rate is high even after surgical treatment. Therefore, drug therapy still plays an irreplaceable role in treating HCE. However, drugs for HCE only exhibit effective therapeutic effects in *in vitro* experiments, which may be due to the complex environment *in vivo*, which limits the efficacy of the drugs [4,5]. Therefore, it is necessary to explore the pathogenesis and pathological changes of HCE and develop novel clinical treatment strategies.

The primary harm of HCE is that it causes and increases hydatid cysts, which compress surrounding tissues, especially liver tissues and intrahepatic ducts, and exerts the corresponding toxic effects, thus aggravating liver damage. In severe cases, hydatid cysts can break into the intrahepatic bile duct system and induce a series of complications, such as jaundice, hydatid cyst infection, and bile duct infection, which threaten the lives of patients [6]. Clinical studies have found that in the growth and development of HCE, the rates of calcification and necrosis of the cyst can be as high as 5–15% [7,8]. Previous studies have demonstrated a correlation between a host immune response and the calcification of the hydatid cyst wall [9,10]. Studies have also shown that the calcification of the outer cyst wall of the hydatid cysts hinders nutrient intake, thereby leading to parasite death [11]. Therefore, inducing and accelerating the hepatic hydatid cyst wall calcification may be a new way to treat HCE.

Calcifying nanoparticles (CNPs), also known as nanobacteria, exist in a variety of human tissues and are spherical ball- or rod-shaped, with diameters ranging from 100 to 600 nm [12]. CNPs are a class of nanoscale protein complexes with bionic properties, such as self-replication, self-mineralization, slow metabolism, and resistance to heat and acid [13,14]. CNPs, which are distributed around the cellular nucleus, may take the human serum fetuin-A as the main component to form nanoscale hydroxyapatite calcification crystals (nano-hydroxy-apatite-collagen [NHAC]) and generate a mineralized shell covering their surroundings to form the crystal core, thus causing pathological calcification of cells and inducing cell injury and death [15,16]. CNPs can secrete calcified lipopolysaccharides, which contribute to a series of inflammatory reactions. Growing evidence indicates that CNPs are associated with the pathological calcification of various human tissues, as well as the occurrence and development of chronic inflammatory diseases, such as coronary artery disease, calcified aortic stenosis, atherosclerosis, kidney stones, gallbladder stones, placental calcification, and chronic periodontitis [17,18]. Moreover, dystrophic calcification caused by pathological changes in the body leads to the formation and accumulation of calcium salts in the cyst wall of cystic hepatic hydatids, which is closely related to local infection, inflammation, and cell damage [19,20]. However, the role of CNPs in the calcification process of the outer cyst wall of HCE and its related mechanisms remain unknown.

Mesenchymal stem cells (MSCs) have been reported to be involved in the formation of the cyst wall of HCE and have osteogenic differentiation ability, which could have the potential to induce the calcification of the HCE wall [21,22]. Therefore, in this study, CNPs were isolated from the calcified outer cyst wall and the contents of the hepatic hydatid. MSCs were used to explore the effects of CNPs on the calcification of the outer cyst wall of the hepatic hydatid and the related underlying mechanisms.

2 Materials and methods

2.1 Patient samples

A total of 37 patients (22 males and 15 females) with HCE were recruited at the First Affiliated Hospital of the Medical College of Shihezi University between January 2018 and December 2018. The mean age of these patients was 43.5 ± 7.6 years. All the patients were diagnosed via computed tomography, and the number, size, location, World Health Organization's image classification, and the hydatid calcification were determined. Postoperative operation was performed to determine whether biliary fistula occurred during and after surgery. Exclusion criteria were the presence of hepatic alveolar echinococcosis, no clinical classification of hepatic hydatids, and no surgical treatment.

Informed consent: Informed consent has been obtained from all individuals included in this study.

Ethical approval: The research related to human use complied with for all the relevant national regulations and institutional policies, is in accordance with the tenets of the Helsinki Declaration, and has been approved by the Institutional Ethics Committee of the First Affiliated Hospital of the Medical College of Shihezi University (approval number: A2017-122-01, date: 2017/3/5).

2.2 Preparation of CNPs and NHAC

The outer cyst wall and contents of the hydatid cysts that were surgically separated from the patient tissues were washed with phosphate-buffered saline (PBS), ground into a homogenate, and incubated with 1 mol/L hydrochloric acid (HCl) at 37°C for 30 min. The pH was adjusted to 7.0–7.4 by adding 1 mol/L Tris-HCl. After the sample had settled naturally, the supernatant was centrifuged at 6,000×*g* for 10 min and then at 14,000×*g* for 40 min at 4°C. The obtained supernatant was sterile-filtered (0.22 μm; Millipore Carrigtwohill, Cork, Ireland) and cultured in RPMI-1640 (Gibco, CA, USA) containing 10% γ-irradiated

fetal bovine serum (FBS; Gibco, CA, USA) at 37°C in a humidified atmosphere of 5% CO_2. After 4 weeks of inoculation, the mixture was centrifuged at 16,000×*g* for 50 min, and the sediments were CNPs. During the 4-week culture, the upper layer of the culture medium was removed every week, and an equal amount of fresh RPMI-1640 medium was added. For cellular analysis, the concentration was adjusted to 3 or 6 MacFarland (MCF) before experimental use. NHAC was purchased from DK Nano Technology, Beijing, China, and dissolved in PBS and sonicated for 6 h to prepare 3.0 MCF NHAC for experimental use.

2.3 CNP morphological analysis

The morphology of the CNPs was examined using transmission electron microscopy (TEM) and scanning electron microscopy (SEM; Hitachi, Tokyo, Japan). For the TEM analysis, the CNPs were fixed in 2.5% glutaraldehyde overnight, resuspended in 0.5 mL ddH_2O, and embedded on a membrane-coated copper screen. Subsequently, the CNPs were dyed with 10 mL/L phosphotungstic acid for 90 s and observed by TEM at 80 kV. For the SEM analysis, the CNPs were fixed in 2.5% glutaraldehyde for 1–2 h and dehydrated by 50, 70, 80, 90, and 100% ethanol gradient treatment for 10 min. Finally, the CNPs were subjected to cryodesiccation and metal coating, and the samples were then subjected to SEM observation.

2.4 Cell culture

Bone marrow-derived MSCs were isolated from C57BL/6 mice (2 weeks old) and identified using common protocols [23]. The prepared MSCs were grown in MEM alpha modification, with L-Glutamine, with ribo- and deoxyribonucleosides (Invitrogen, CA, USA) supplemented with 100 U/mL penicillin/streptomycin (Invitrogen) and 20% FBS, and were maintained at 37°C in a 5% CO_2 atmosphere. For analysis, cultured MSCs were divided into four groups: control group, NHAC group (3 MCF), low-CNP group (L-CNP, 3 MCF), and high-CNP group (H-CNP, 6 MCF). The mouse experiments were conducted in accordance with the National Medical Advisory Committee (NMAC) guidelines, and the approved procedures of the Institutional Animal Care and Use Committee at the First Affiliated Hospital of Medical College of Shihezi University were employed (approval number: A2017-122-01, date: 2017/3/5).

2.5 CCK-8 cell viability assay

MSCs in the logarithmic growth phase were seeded into 96-well plates at a density of 2×10^3 cells per well and treated with PBS, NHAC (3.0 MCF), L-CNPs (3.0 MCF), and H-CNPs (6.0 MCF). At 3 and 6 days post-treatment, 10 µL of CCK-8 solution (Beyotime Biotechnology, Shanghai, China) was added to the culture medium and incubated at 37°C for 6 h, after which the optical density at 450 nm was measured using a microplate spectrophotometer (Bio-Rad, CA, USA).

2.6 Apoptosis assay

Cultured MSCs from the different treatment groups were harvested via centrifugation at 1,000×*g* for 5 min and resuspended in 100 µL of 1× binding buffer, followed by incubation with Annexin V-FITC/PI (BD Biosciences, NJ, USA) at 4°C for 30 min in the dark according to the manufacturer's instructions. MSC apoptosis was determined using a flow cytometer (BD Biosciences).

2.7 Western blot

MSCs from the different treatment groups were harvested and lysed in ice-cold RIPA buffer (Beyotime Biotechnology, Shanghai, China) supplemented with 1 mM PMSF (Millipore Carrigtwohill, Cork, Ireland). The total extracted protein was quantified using a BCA Protein Assay Kit (Beyotime Biotechnology, Shanghai, China) and fractionated by SDS-PAGE. The separated proteins were transferred onto polyvinylidene difluoride (Millipore Carrigtwohill, Cork, Ireland) membranes, followed by blocking in 5% non-fat milk for 1 h at room temperature. Subsequently, the membrane was incubated with primary anti-RUNX2 antibody (1:1,000; Abcam), anti-OPN antibody (1:1,000; Abcam), anti-BMP-2 antibody (1:1,000; Abcam), anti-GAPDH antibody (1:1,000; Hangzhou Xianzhi Biological Co., Ltd.), anti-caspase-3 antibody (1:2,000; NOVUS), anti-Bcl-2 antibody (1:1,000; Proteintech Group, Inc.), anti-Bax antibody (1:1,000; Abcam), anti-Smad3 antibody (1:1,000; Abcam), and anti-TGF-β1 antibody (1:1,000; Proteintech Group, Inc.) overnight at 4°C. The membrane was thereafter incubated with the corresponding horseradish peroxidase-linked secondary antibodies (1:5,000; Wuhan Boster Biological Technology Co., Ltd) at room temperature for 1 h. The expression and images of protein bands were visualized and recorded using an ECL Plus Western Blotting Detection System (Bio-Rad, CA, USA).

2.8 Immunofluorescence assays

MSCs from the different treatment groups were fixed with 4% formaldehyde for 10 min, followed by 1% BSA incubation for 1 h at room temperature. After washing three times with PBS, the MSCs were probed at room temperature with the corresponding primary antibodies for 2 h. Then, the MSCs were incubated with secondary antibodies and DAPI for 1 h in the dark. Finally, the MSCs were washed with PBS, and images were taken using a fluorescence microscope.

2.9 Calcium ion deposition detection

Calcium ion deposition in MSCs from the different treatment groups was determined by alkaline phosphatase (ALP) staining and alizarin red S staining. ALP staining was performed using an alkaline phosphatase staining kit II (Stemgent, MA, USA) according to the manufacturer's instructions. Alizarin-Red S staining analysis was conducted following the commercial guidelines (Solarbio Life Science, Beijing, China). The remaining Alizarin Red S solution was removed, after which the samples were observed, and the images were recorded under a microscope.

2.10 Statistical analysis

Data are presented as mean ± standard deviation (SD). Categorical data were expressed as frequencies and percentages. Statistical analysis was conducted using SPSS 21.0 (IBM, IL, USA) software, and GraphPad Prism 5 (GraphPad Software, San Diego, CA, USA) was used for figure plotting. Student's *t*-test was employed for comparisons between two groups. One-way analysis of variance followed by a *post-hoc* Tukey test was used for comparisons among at least three groups. The threshold for statistical significance was set at $P < 0.05$.

3 Results

3.1 CNP ultrastructural morphology

According to the TEM observations, the cultured CNPs displayed a coccoid form with diameters ranging from 100 to 600 nm (Figure 1a–d), which indicated that the CNPs were involved in the splitting process of binary fission. Furthermore, SEM analysis revealed that the CNPs were of different sizes, with a certain degree of black compactness on the outer periphery, and that the inside was a concentric ring structure (Figure 1e–h). Both TEM and SEM revealed that the surfaces of the particles were uneven, with crystals resembling burrs, implying that the CNPs were successfully isolated from the tissues of patients with HCE.

3.2 CNPs promoted the expression of calcification-related proteins in MSCs

In order to investigate the effects of CNPs on the differentiation of MSCs, we examined the expression of calcification-related proteins, such as bone morphogenetic protein-2 (BMP-2) and osteopontin (OPN), in MSCs subjected to different treatments. As shown in the immunofluorescence assays and western blot experiments, the protein levels of BMP and OPN were markedly upregulated in the CNP group in a dose-dependent manner compared with those in the control and NAHC groups ($P < 0.05$, Figure 2). Additionally, as a nuclear transcription factor, RUNX2 plays a critical role in chondrocyte differentiation and osteoblast formation [24]. Our western blot assay revealed that the protein expression of RUNX2 was greatly upregulated by CNP treatment, and that the RUNX2 level was positively correlated with the concentration of CNPs ($P < 0.05$, Figure 2c and d).

3.3 CNPs accelerated the calcification process of MSCs

To investigate the effect of CNPs on ALP activity, we analyzed the ALP activity in MSCs from the different treatment groups. It was found that the ALP level in the NHAC group was higher than that of the control group, and the CNP group exhibited the highest level of ALP (Figure 3a). To further confirm the roles of CNPs in the calcification of MSCs, calcium ion deposition and the fluorescence intensity of calcium ions in MSCs were quantitatively analyzed via alizarin-red S staining and flow cytometry. Compared with the control group, both the NAHC and CNP groups showed significant calcium ion deposition, and the MSCs incubated with CNP had the highest calcium ion deposition ($P < 0.05$, Figure 3b and c). In addition, with an increase in the concentration of CNPs, the calcium ion concentration in MSCs also significantly

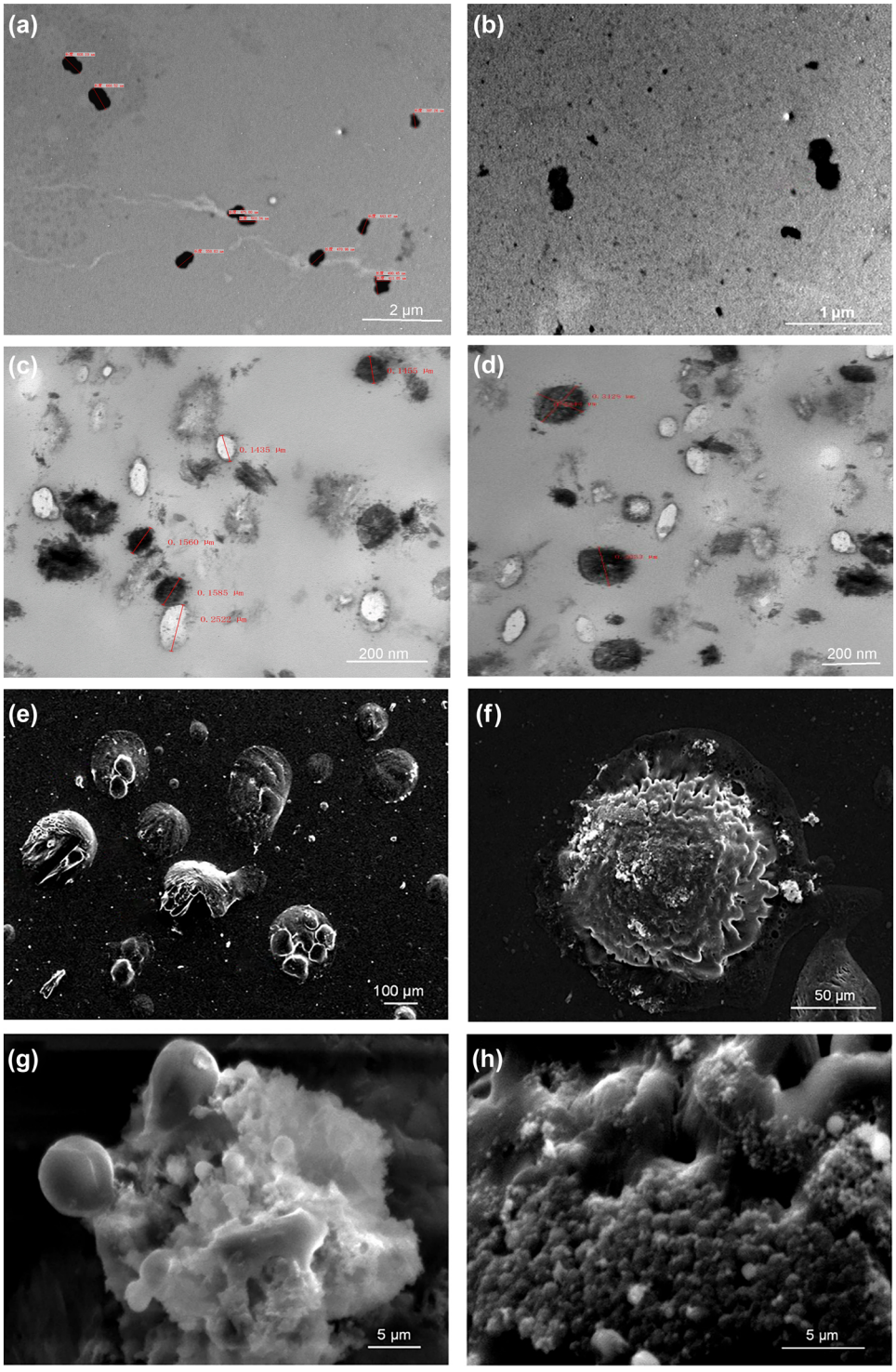

Figure 1: The ultrastructural morphology of CNPs observed using TEM and SEM. (a–d) The TEM images of CNP isolates under different magnification times. (e–h) The SEM images of CNP isolates under different magnification times.

increased in a dose-dependent manner. These results imply that the CNPs could promote calcium deposition and calcium concentration in MSCs, thereby accelerating the process of MSC calcification.

3.4 CNPs induced MSC apoptosis *in vitro*

To detect the effects of the CNPs on the MSC proliferation, CCK-8 analysis was performed. As presented in Figure 4a,

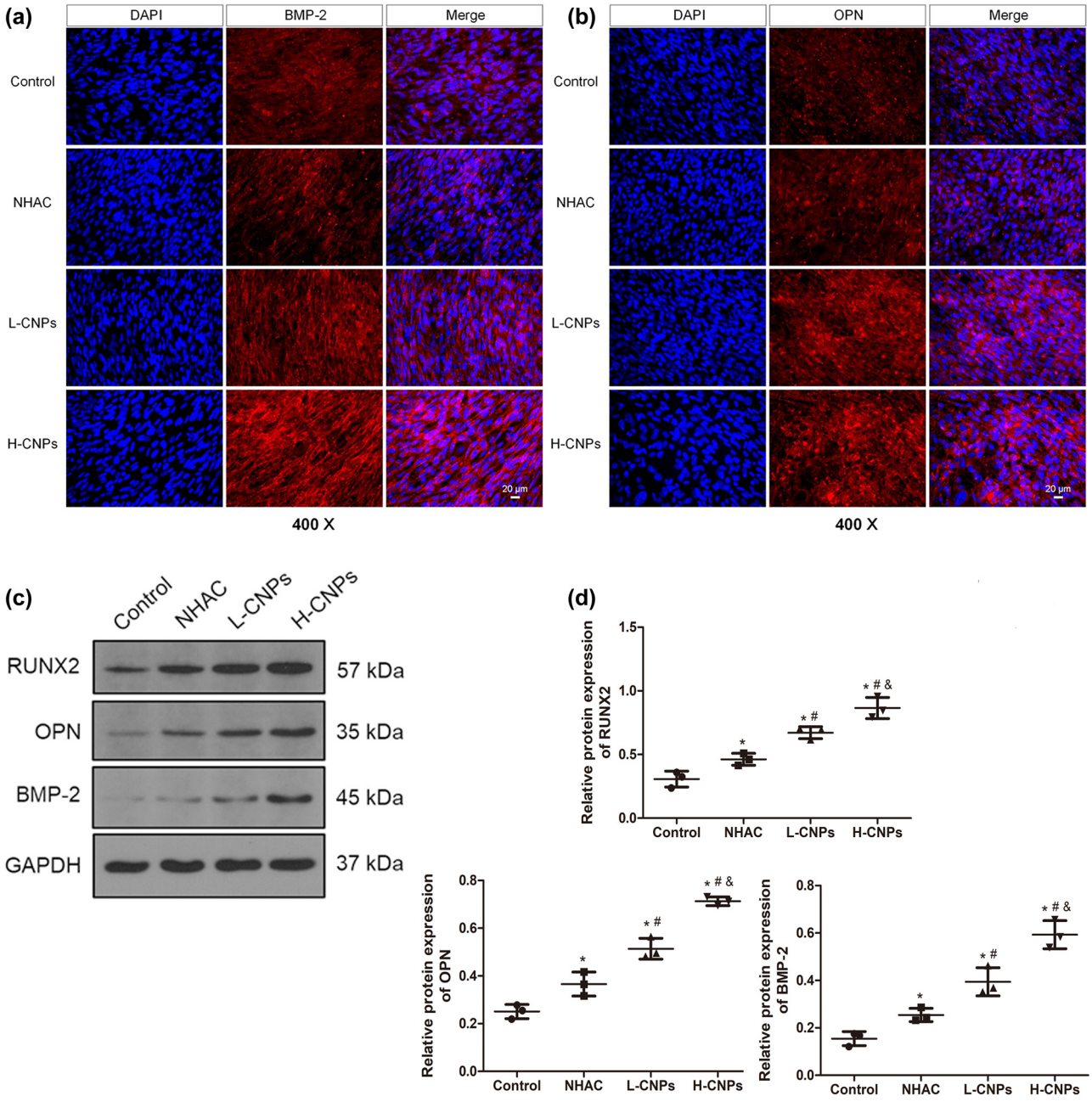

Figure 2: Effects of CNPs on calcification-related proteins, including BMP-2, OPN, and RUNX2 in MSCs after 6 days of co-culture. (a) BMP-2 protein expression was determined using immunofluorescence assays. (b) OPN protein expression was measured using immunofluorescence assays. (c) Protein bands of BMP-2, OPN, and RUNX2 were visualized by western blotting. (d) The gray values of BMP-2, OPN, and RUNX2 were quantified using ImageJ software. $^{*}P < 0.05$, compared to the control group; $^{\#}P < 0.05$, compared to the NHAC group; and $P < 0.05$, compared to the L-CNP group.

compared with the control and NHAC groups, treatment with CNPs significantly inhibited the proliferation rate of MSCs ($P < 0.05$), and this inhibitory effect was dependent on the concentration and treatment duration. In addition, flow cytometric analysis revealed that CNP treatment markedly increased the apoptotic rate of MSCs in a concentration-dependent manner ($P < 0.05$; Figure 4b and c). Incubation with CNPs led to a larger number of MSCs in both early and late apoptosis compared to that in the control and NHAC groups (Figure 4c). Similar results were obtained in the western blot assays. CNP exposure induced higher protein expression of pro-apoptotic

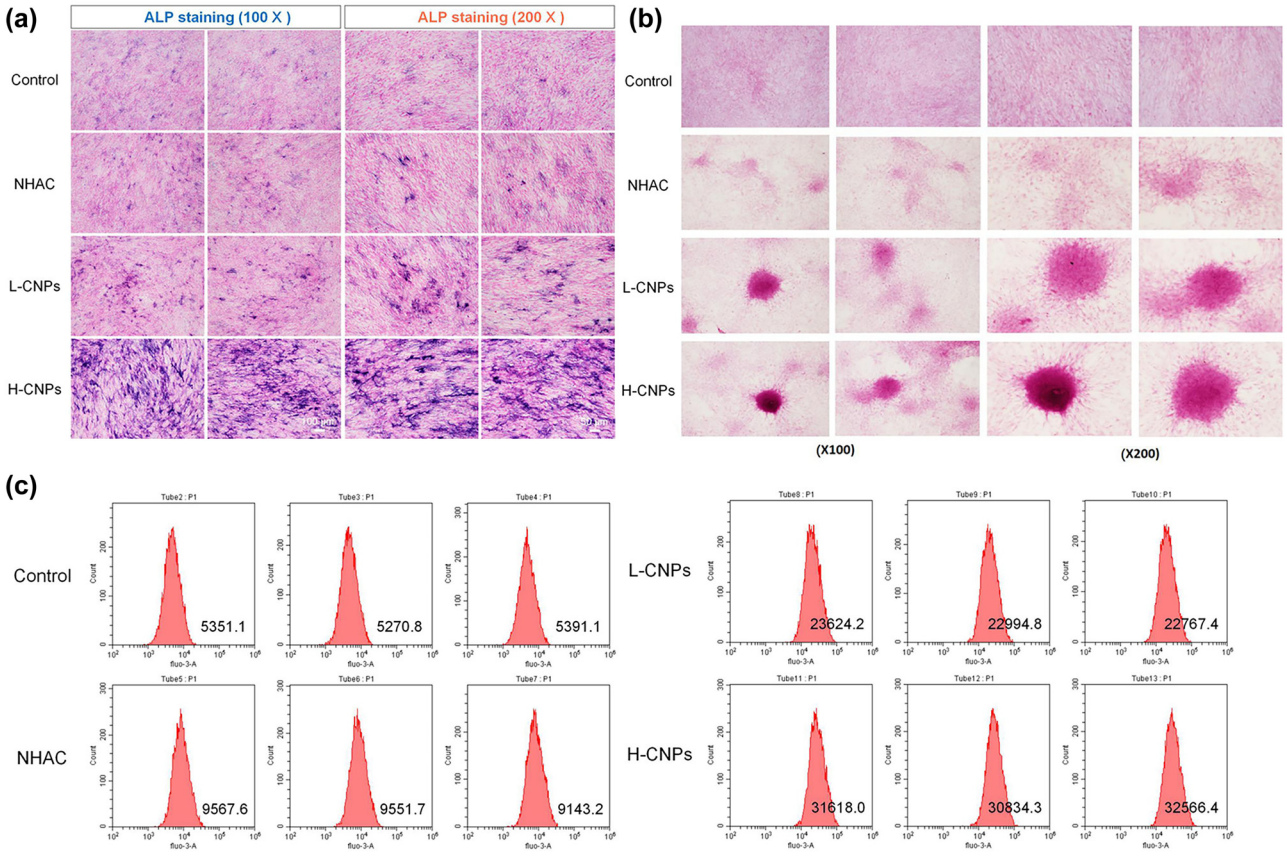

Figure 3: Effects of CNPs on calcium ion deposition in MSCs. (a) ALP staining analysis of MSCs from different treatment groups. (b) Alizarin red S staining was used to analyze calcium deposition in MSCs after different treatments. (c) Fluorescence intensity of calcium ions in MSCs from different treatment groups was quantified using flow cytometry.

factors, such as Bax and Caspase-3, and suppressed Bcl-2 expression (Figure 4d). These results indicate that CNPs contribute to the apoptosis of MSCs *in vitro*.

3.5 CNPs activate the TGF-β signaling pathway to induce the calcification of MSCs

The transforming growth factor-β1 (TGF-β1)/Smad3 signaling pathway plays a critical role in the process of liver fibrosis and the regulation of tissue cell calcification. In the present study, western blot assays revealed that the expression of TGF-β1 and Smad3 was significantly upregulated in the MSCs treated with CNPs, compared with that in the NHAC group ($P < 0.05$), and that TGF-β1 and Smad3 exhibited the lowest expression levels in the control group (Figure 5). These results suggest that CNPs can activate the TGF-β signaling pathway in MSCs *in vitro*.

4 Discussion

In the current study, to explore the effects of CNPs on the calcification process of the outer cyst wall of HE, we first isolated and cultured CNPs from HE cyst wall tissue and identified these particles by TEM and SEM. To eliminate false-positive results, we ensured that there were no suspected particles in the reagents and consumables used during isolation and culture. All metal instruments and glassware applied in the test were used after sterilization, and the specimens were collected in strict accordance with aseptic operations. Under TEM, we observed that these nanoparticles were covered by a dense and burr-like outer shell, which was similar to the previously reported morphological characteristics [25–27]. SEM revealed that crystals existed on the surfaces of the nanoparticles, which confirmed that the CNPs had been successfully isolated and could be used for further cellular experiments.

The outer cyst wall of the HCE is mainly composed of fibroblasts. Like osteoblasts, fibroblasts can produce matrix vesicles and induce calcium salt deposition in the vesicles,

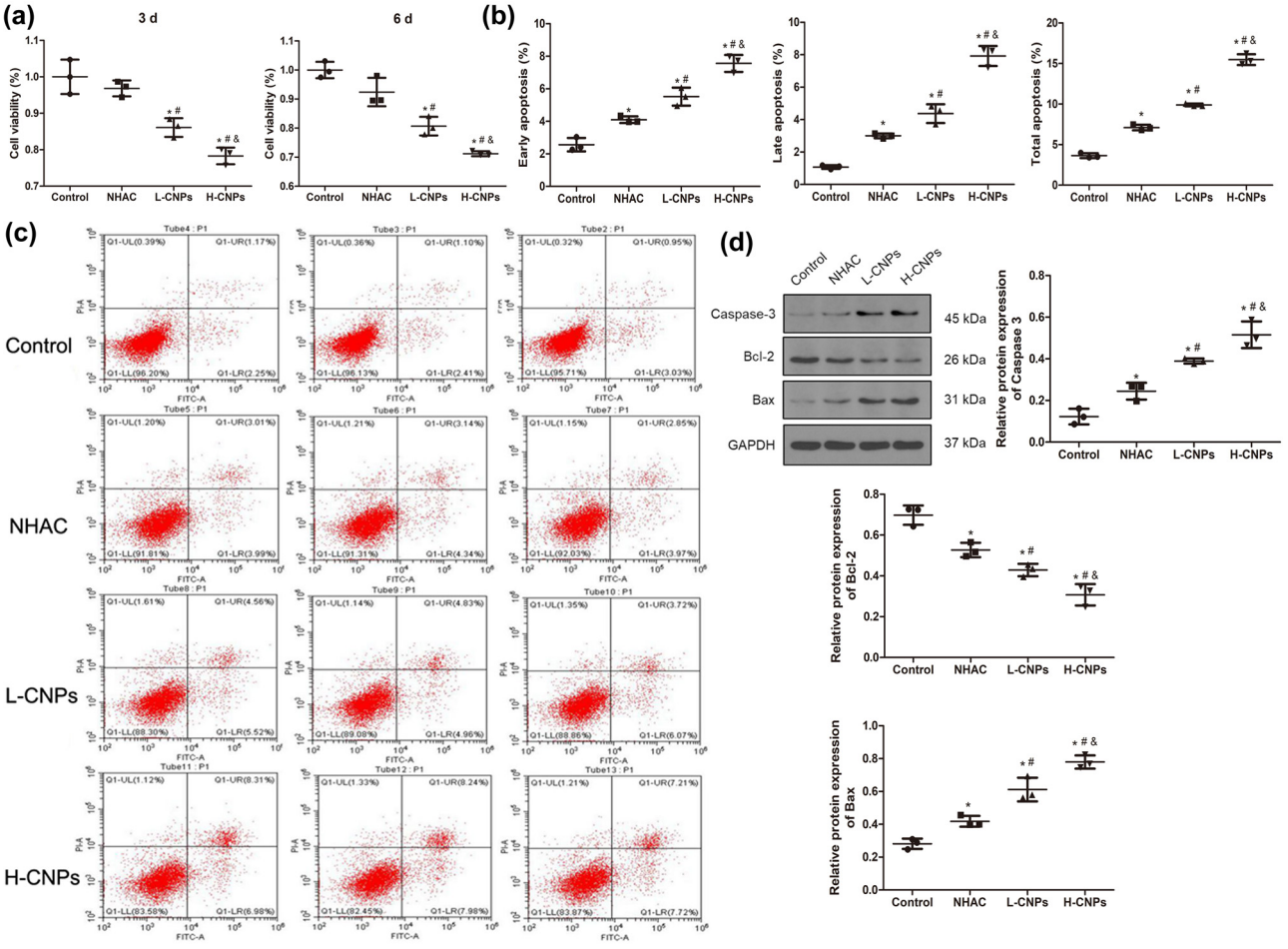

Figure 4: Effects of CNPs on the proliferation and apoptosis of MSCs *in vitro*. (a) The growth of MSCs in control, NHAC, L-CNP, and H-CNP groups was measured using a CCK-8 assay. (b) Early apoptosis rates in the MSCs with different treatments were calculated. (c) The apoptosis of MSCs from different treatment groups was analyzed using flow cytometry. $^{**}P < 0.01$; $^{***}P < 0.001$, compared to the control group. (d) The expression of apoptosis-related proteins (Caspase-3, Bcl2, and Bax) detected by western blotting. The panel below represents the gray values of protein bands. $^{*}P < 0.05$, compared to the control group; $^{\#}P < 0.05$, compared to the NHAC group; and $P < 0.05$, compared to the L-CNP group.

suggesting that the calcification of the fibrous cyst wall around the hepatic hydatid may be related to the mechanism of bone formation [28]. In addition, MSCs can contribute to the formation of cyst walls in HCE [29]. Therefore, we selected MSCs with osteogenic phenotypic potential as co-culture objects to explore the effects of the CNPs on the MSC osteogenic calcification, and then investigated the potential mechanism of CNP-induced calcification of the hepatic hydatid outer capsule wall.

Furthermore, to investigate the effects of CNPs on the differentiation of MSCs, the MSCs were treated with different concentrations of CNPs, and the expression levels of calcification-related proteins (BMP-2, OPN, and RUNX2) were determined. The main component of the CNPs is hydroxyapatite, which can promote bone formation and the secretion of calcification-related proteins [30]. OPN is a highly phosphorylated glycoprotein that plays a critical role in cardiovascular diseases, kidney stone diseases, and biological mineralization [31]. RUNX2 has been reported to play a key role in the chondrocyte differentiation and osteoblast formation, as well as in the regulation of osteoblast differentiation and the triggering of bone matrix protein expression [32]. Moreover, BMP-2 can promote the differentiation of hepatic hydatid cyst wall cells into osteoblasts. In addition, MSCs can generate BMP-2 via autocrine/paracrine secretion and elevate RUNX2 expression, all of which accelerate calcification [33,34]. These factors can induce calcium salt deposition in MSCs and trigger the formation of calcified cyst walls in hepatic hydatids. Additionally, previous studies have shown that

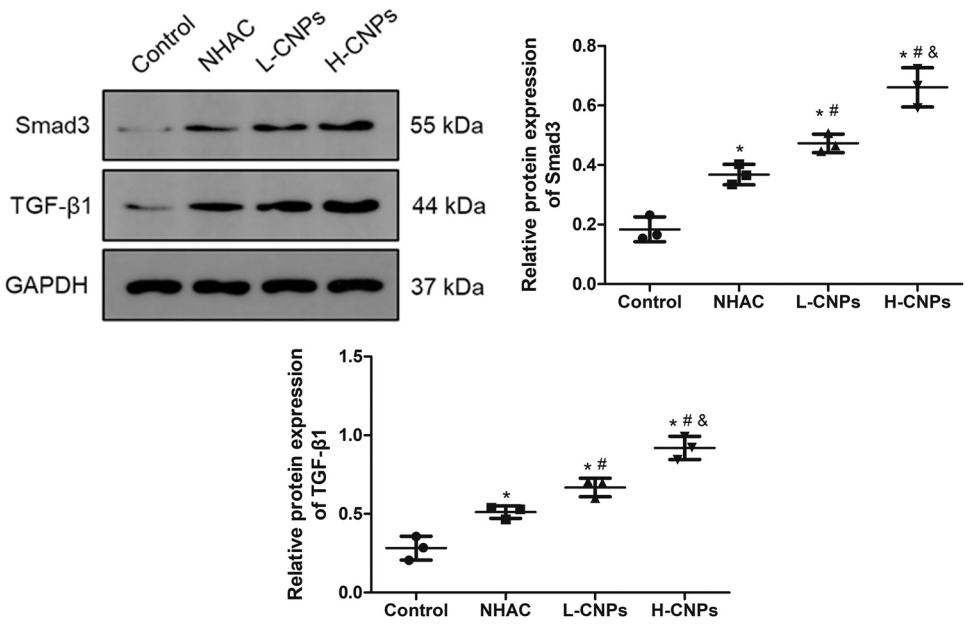

Figure 5: The protein expression of TGF-β1 and Smad3 evaluated by western blotting. *$P < 0.05$, compared to the control group; $^{\#}P < 0.05$, compared to the NHAC group; and $P < 0.05$, compared to the L-CNP group.

the CNPs could promote the differentiation of MSCs into osteoblasts, and the CNPs' microenvironment may be crucial for the MSC differentiation and calcification [13,35]. Our quantitative analyses revealed that the CNPs increased the protein levels of BMP-2, OPN, and RUNX2 in MSCs in a dose-dependent manner, indicating that CNPs may act as inducers to differentiate MSCs into osteoblast-like cells and indirectly promote calcification.

Collagen fibers have a certain affinity for ALP, which can effectively accelerate the accumulation of phosphates and initiate calcification [36–38]. According to our staining results, incubation with the CNPs significantly upregulated the ALP activity in MSCs. Additionally, alizarin-red S staining and flow cytometric analysis demonstrated that the CNP treatment significantly increased the calcium ion deposition in MSCs, confirming that CNPs could facilitate calcium deposition in MSCs and accelerate the process of cell calcification.

Apoptosis is considered one of the major mechanisms of cardiovascular calcification, particularly the adverse calcification caused by atherosclerosis [39,40]. Calcified cardiovascular valves are caused by a combination of apoptotic bodies, death organelles, senescent cells, and many cell fragments with calcium, gradually resulting in calcium deposition [41,42]. In this study, both CCK-8 and flow cytometry experiments confirmed that the CNP treatment promoted MSC apoptosis. Pro-apoptotic factors such as Bax and Caspase-3 displayed higher expression in the CNP groups than in the control group, while the apoptosis inhibitor Bcl-2 was downregulated by the CNP treatment. Taken together, we hypothesized that the accumulation of cell debris generated by the CNPs could induce MSC apoptosis and that calcified nanoparticles could form a mineralized core. Together with the calcium metabolism disorder caused by hydroxyapatite, they can jointly induce the calcification of the cyst wall cells. Increased calcification may hinder the cells' access to nutrients, leading to local metabolic disorders of the cells, which in turn leads to apoptosis [13,43].

It has been reported that TGF-β is expressed in the outer cyst wall tissue of the hepatic cystic hydatid [44]. TGF-β is not only involved in the process of liver fibrosis but also participates in cell calcification and apoptosis [45]. Smad transduces the TGF-β receptor signal into the nucleus [46] and initiates the transcription of downstream targeted genes, which play an important role in TGF-β1-mediated liver fibrosis [47–49]. In our study, we observed that TGF-β1 and Smad expression was elevated under the CNP treatment, which indicated that CNPs may effectively activate the TGF-β1/Smad3 signaling pathway and further accelerate the calcification process of MSCs.

Interestingly, NHAC also affects the proliferation, apoptosis, calcification, and other aspects of MSCs [50]. However, the action of the MSCs treated with the CNPs was significantly affected compared with that of NHAC-

induced MSCs. Although the main component of CNPs is hydroxyapatite, CNPs have a stronger calcification induction effect than NHAC alone. This may be related to the toxicity of the CNPs, which requires further research.

This study had some limitations. First, the frequency of the diameter, specific composition, and the biomechanical and physicochemical properties of the CNPs should be determined in the following studies. Second, the expression of phospho-Smad1/5 and phospho-Smad3 needs to be further examined, and the potential modulatory effects of CNPs on distinct mesenchymal stem cell differentiation pathways require further investigation. Additionally, further experiments will be performed to investigate deeper mechanics through interference experiments (knockdown or overexpression) or the effects of different time points on MSCs and gene/protein expression.

5 Conclusion

In conclusion, CNPs from the calcified outer cyst wall of cystic hepatic hydatids may serve as calcification inducers, leading to calcium ion deposition in MSCs by upregulating the expression of calcification-related proteins (BPM-2, OPN, and RUNX2). In addition, CNPs may promote the differentiation of MSCs into osteoblast-like cells and induce apoptosis of MSCs by activating the TGF-β1/Smad3 signaling pathway, thus persistently causing calcium metabolism disorder in cells and aggravating surface cell calcification. The findings of our study also indicate that the CNPs may be an important factor in initiating the calcification of the outer cyst wall of HCE and promoting the decline of hydatid cysts. This study provides a new research direction for further investigation of the natural course and the clinical treatment of HCE.

Funding information: This study was supported by the Non-profit Central Research Institute Fund of the Chinese Academy of Medical Sciences (2020-PT330-003).

Author contributions: Conceptualization, Xiangwei Wu and Xinyu Peng; data curation, Jian Yang; formal analysis, Jian Yang and Meiyan Wang; funding acquisition, Xiangwei Wu; investigation, Jian Yang, Jing Yang, Zhiqiang Chu, and Xueling Chen; methodology, Jian Yang and Xueling Chen; project administration, Jian Yang; resources, Xiangwei Wu and Xinyu Peng; software, Meiyan Wang; supervision, Xinyu Peng; validation, Jing Yang and Zhiqiang Chu; visualization, Jing Yang and Zhiqiang Chu; writing – original draft, Jian Yang; writing – review and editing, Xiangwei Wu and Xinyu Peng.

Conflict of interest: Authors state no conflict of interest.

Data availability statement: The datasets generated during and/or analyzed during the current study are available from the corresponding author on reasonable request.

References

[1] Dehkordi AB, Sanei B, Yousefi M, Sharafi SM, Safarnezhad F, Jafari R, et al. Albendazole and treatment of hydatid cyst: review of the literature. Infect Disord Drug Targets. 2019;19(2):101–4.
[2] Brunetti E, Tamarozzi F, Macpherson C, Filice C, Piontek MS, Kabaalioglu A, et al. Ultrasound and cystic echinococcosis. Ultrasound Int Open. 2018;4(3):E70–8.
[3] Tamarozzi F, Akhan O, Cretu CM, Vutova K, Fabiani M, Orsten S, et al. Epidemiological factors associated with human cystic echinococcosis: a semi-structured questionnaire from a large population-based ultrasound cross-sectional study in eastern Europe and Turkey. Parasit Vectors. 2019;12(1):371.
[4] Siles-Lucas M, Casulli A, Cirilli R, Carmena D. Progress in the pharmacological treatment of human cystic and alveolar echinococcosis: Compounds and therapeutic targets. PLoS Negl Trop Dis. 2018;12(4):e0006422.
[5] Yu XK, Zhang L, Ma WJ, Bi WZ, Ju SG. An Overview of Hepatic Echinococcosis and the Characteristic CT and MRI Imaging Manifestations. Infect Drug Resist. 2021;14:4447–55.
[6] Castillo S, Manterola C, Grande L, Rojas C. Infected hepatic echinococcosis. Clinical, therapeutic, and prognostic aspects. A systematic review. Ann Hepatol. 2021;22:100237.
[7] Labsi M, Soufli I, Khelifi L, Amir ZC, Touil-Boukoffa C. In vivo treatment with IL-17A attenuates hydatid cyst growth and liver fibrogenesis in an experimental model of echinococcosis. Acta Trop. 2018;181:6–10.
[8] Peng X, Li J, Wu X, Zhang S, Niu J, Chen X, et al. Detection of Osteopontin in the pericyst of human hepatic Echinococcus granulosus. Acta Trop. 2006;100(3):163–71.
[9] Gottstein B, Soboslay P, Ortona E, Wang J, Siracusano A, Vuitton D. Immunology of alveolar and cystic echinococcosis (AE and CE). Adv Parasitol. 2017;96:1–54.
[10] Rogan MT, Bodell AJ, Craig PS. Post-encystment/established immunity in cystic echinococcosis: is it really that simple? Parasite Immunol. 2015;37(1):1–9.
[11] Woolsey ID, Miller AL. Echinococcus granulosus sensu lato and Echinococcus multilocularis: A review. Res Vet Sci. 2021;135:517–22.
[12] Zeper LW, de Baaij JHF. Magnesium and calciprotein particles in vascular calcification: the good cop and the bad cop. Curr Opnephrol Hypert. 2019;28(4):368–74.
[13] Can Demirdöğen B. Potential role of calcifying nanoparticles in the etiology of multiple sclerosis. Med Hypoth. 2019;128:25–7.

[14] Wu J, Tao Z, Deng Y, Liu Q, Liu Y, Guan X, et al. Calcifying nanoparticles induce cytotoxicity mediated by ROS-JNK signaling pathways. Urolithiasis. 2019;47(2):125–35.
[15] Atmaca HT, Gazyagci AN, Terzi OS, Sumer T. Role of stellate cells in hepatic echinococcosis in cattle. J Parasit Dis. 2019;43(4):576–82.
[16] Kang MK, Kim KH, Choi JH. Hepatic cystic echinococcosis due to Echinococcus granulosus, grossly observed by needle aspiration. Korean J Intern Med. 2019;34(6):1394–5.
[17] Fayez Hassan N, Khaled Ibrahim M, Yousef El Tablawy S, Abd Allah Farrag H. Characterization of biofilm producer nanobacteria isolated from kidney stones of some Egyptian patients. Pak J Biol Sci PJBS. 2021;24(9):953–70.
[18] Sardarabadi H, Mashreghi M, Jamialahmadi K, Matin MM, Darroudi M. Selenium nanoparticle as a bright promising anti-nanobacterial agent. Microb Pathog. 2019;126:6–13.
[19] Chaiin P, Yostaworakul J, Rungnim C, Khemthong P, Yata T, Boonrungsiman S. Self-calcifying lipid nanocarrier for bone tissue engineering. Biochim Biophys Acta Gen Subj. 2022;1866(2):130047.
[20] Chin DD, Wang J, Mel de Fontenay M, Plotkin A, Magee GA, Chung EJ. Hydroxyapatite-binding micelles for the detection of vascular calcification in atherosclerosis. J Mater Chem B. 2019;7(41):6449–57.
[21] Wilson CS, Jenkins DJ, Barnes TS, Brookes VJ. Evaluation of the diagnostic sensitivity and specificity of meat inspection for hepatic hydatid disease in beef cattle in an Australian abattoir. Prev Vet Med. 2019;167:9–15.
[22] Zhang Y, Zhu R, Liu D, Gong M, Hu W, Yi Q, et al. Tetracycline attenuates calcifying nanoparticles-induced renal epithelial injury through suppression of inflammation, oxidative stress, and apoptosis in rat models. Transl Androl Urol. 2019;8(6):619–30.
[23] Otsuka-Yamaguchi R, Kitada M, Kuroda Y, Kushida Y, Wakao S, Dezawa M. Isolation and characterization of bone marrow-derived mesenchymal stem cells in Xenopus laevis. Stem Cell Res. 2021;53:102341.
[24] Komori T. Runx2, an inducer of osteoblast and chondrocyte differentiation. Histochem Cell Biol. 2018;149(4):313–23.
[25] Altundag K. Association between nanobacteria and microcalcifications in breast. J buon. 2021;26(1):280–1.
[26] Lin XC, Gao X, Lu GS, Song B, Zhang QH. Role of calcifying nanoparticles in the development of testicular microlithiasis in vivo. BMC Urol. 2017;17(1):99.
[27] Wu JH, Deng YL, Liu Q, Yu JC, Liu YL, He ZQ, et al. Induction of apoptosis and autophagy by calcifying nanoparticles in human bladder cancer cells. Tumour Biol J Int Soc Oncodev Biol Med. 2017;39(6):1010428317707688.
[28] Jiménez M, Stoore C, Hidalgo C, Corrêa F, Hernández M, Benavides J, et al. Lymphocyte populations in the adventitial layer of hydatid cysts in cattle: relationship with cyst fertility status and fasciola hepatica co-infection. Vet Pathol. 2020;57(1):108–14.
[29] Shams M, Javanmardi E, Nosrati MC, Ghasemi E, Shamsinia S, Yousefi A, et al. Bioinformatics features and immunogenic epitopes of Echinococcus granulosus Myophilin as a promising target for vaccination against cystic echinococcosis. Infect Genet Evol. 2021;89:104714.
[30] Vimalraj S. Alkaline phosphatase: Structure, expression and its function in bone mineralization. Gene. 2020;754:144855.
[31] Si J, Wang C, Zhang D, Wang B, Zhou Y. Osteopontin in bone metabolism and bone diseases. Med Sci Monit. 2020;26:e919159.
[32] Kim WJ, Shin HL, Kim BS, Kim HJ, Ryoo HM. RUNX2-modifying enzymes: therapeutic targets for bone diseases. Exp Mol Med. 2020;52(8):1178–84.
[33] Halloran D, Durbano HW, Nohe A. Bone Morphogenetic Protein-2 in Development and Bone Homeostasis. J Develop Biol. 2020;8:3.
[34] Han S, Paeng KW, Park S, Jung UW, Cha JK, Hong J. Programmed BMP-2 release from biphasic calcium phosphates for optimal bone regeneration. Biomaterials. 2021;272:120785.
[35] Zhang SM, Tian F, Jiang XQ, Li J, Xu C, Guo XK, et al. Evidence for calcifying nanoparticles in gingival crevicular fluid and dental calculus in periodontitis. J Periodontol. 2009;80(9):1462–70.
[36] Lee SJ, Lee IK, Jeon JH. Vascular calcification-new insights into its mechanism. Int J Mol Sci. 2020;21(8):2685.
[37] Ma WQ, Sun XJ, Zhu Y, Liu NF. Metformin attenuates hyperlipidaemia-associated vascular calcification through anti-ferroptotic effects. Free Radic Biol Med. 2021;165:229–42.
[38] Yuan C, Ni L, Zhang C, Hu X, Wu X. Vascular calcification: New insights into endothelial cells. Microvas Res. 2021;134:104105.
[39] Rogers MA, Aikawa E. Cardiovascular calcification: artificial intelligence and big data accelerate mechanistic discovery. Nat Rev Cardiol. 2019;16(5):261–74.
[40] Wang SS, Wang C, Chen H. MicroRNAs are critical in regulating smooth muscle cell mineralization and apoptosis during vascular calcification. J Cell Mol Med. 2020;24(23):13564–72.
[41] Durham AL, Speer MY, Scatena M, Giachelli CM, Shanahan CM. Role of smooth muscle cells in vascular calcification: implications in atherosclerosis and arterial stiffness. Cardiovasc Res. 2018;114(4):590–600.
[42] Li W, Su SA, Chen J, Ma H, Xiang M. Emerging roles of fibroblasts in cardiovascular calcification. J Cell Mol Med. 2021;25(4):1808–16.
[43] Young JD, Martel J, Young D, Young A, Hung CM, Young L, et al. Characterization of granulations of calcium and apatite in serum as pleomorphic mineralo-protein complexes and as precursors of putative nanobacteria. PLoS One. 2009;4(5):e5421.
[44] Tian F, Liu Y, Gao J, Yang N, Shang X, Lv J, et al. Study on the association between TGF-beta1 and liver fibrosis in patients with hepatic cystic echinococcosis. Exp Ther Med. 2020;19(2):1275–80.
[45] Yang P, Troncone L, Augur ZM, Kim SSJ, McNeil ME, Yu PB. The role of bone morphogenetic protein signaling in vascular calcification. Bone. 2020;141:115542.
[46] Hu HH, Chen DQ, Wang YN, Feng YL, Cao G, Vaziri ND, et al. New insights into TGF-β/Smad signaling in tissue fibrosis. Chem-Biol Interact. 2018;292:76–83.
[47] Chen Y, Di C, Zhang X, Wang J, Wang F, Yan JF, et al. Transforming growth factor β signaling pathway: A promising therapeutic target for cancer. J Cell Physiol. 2020;235(3):1903–14.
[48] Ongaro L, Schang G, Ho CC, Zhou X, Bernard DJ. TGF-β superfamily regulation of follicle-stimulating hormone synthesis by

gonadotrope cells: is there a role for bone morphogenetic proteins? Endocrinology. 2019;160(3):675–83.

[49] Zhang T, Wang XF, Wang ZC, Lou D, Fang QQ, Hu YY, et al. Current potential therapeutic strategies targeting the TGF-β/Smad signaling pathway to attenuate keloid and hypertrophic scar formation. Biomed Pharmacother. 2020;129:110287.

[50] Hassanzadeh A, Ashrafihelan J, Salehi R, Rahbarghazi R, Firouzamandi M, Ahmadi M, et al. Development and biocompatibility of the injectable collagen/nano-hydroxyapatite scaffolds as in situ forming hydrogel for the hard tissue engineering application. Artif Cells Nanomed Biotechnol. 2021;49(1):136–46.